Observing the Superconducting State of HgBa$_2$Ca$_2$Cu$_3$O$_{8+\delta}$ Cuprate by Electronic Raman Scattering

B. Loret[1], A. Sacuto[1], D. Colson[2], Y. Gallais[1], M. Cazayous[1], M.-A. Méasson[1] and A. Forget[2]

[1] *Laboratoire Matériaux et Phénomènes Quantiques (UMR 7162 CNRS),*
Université Paris Diderot-Paris 7, Bat.Condorcet, 75205 Paris Cedex 13, France,
[2] *Service de Physique de l'État Condensé, DSM/IRAMIS/SPEC (UMR 3680 CNRS),*
CEA Saclay 91191 Gif sur Yvette cedex France.
(Dated: August 27, 2015)

Electronic Raman scattering with in and out of (ab) plane polarizations have been performed on HgBa$_2$Ca$_2$Cu$_3$O$_{8+\delta}$ in a slightly underdoped single crystal with a critical temperature T$_c$=122 K. We find that the d-wave pairing gap at the antinodes is higher in energy (14 k_BT$_c$) than in other cuprates and that it varies very slowly up to T_c. This hints at a strong coupling nature of the pairing mechanism. Interestingly, we reveal that the pairing-gap feature in the Raman response displays a complex peak-dip-hump structure, in a fashion reminiscent of what observed by angle resolved photo-emission spectroscopy in Bi$_2$Sr$_2$CaCu$_2$O$_{8+\delta}$ (Bi-2212). We detect two other distinct superconducting peaks at $\approx 5k_B$T$_c$ and $\approx 7k_B$T$_c$ when probing respectively around the nodes and on the whole Fermi surface. Finally we establish that the pairing gap at the antinodes is detected both for (ab) plane and for c-axis light polarizations. This shows that the quasiparticle dynamics along the c-axis is intimately connected to the antinodal one in the (ab) plane.

I. INTRODUCTION

The discovery of the three-copper-oxide-layer compound HgBa$_2$Ca$_2$Cu$_3$O$_{8+\delta}$ (Hg-1223) by A. Schilling et al.[1] in 1993 was a breakthrough in the quest of high critical temperature superconductors. Indeed, the Hg-1223 cuprate exhibits a critical temperature T_c of 135 K at ambient pressure, i.e. 40 K higher than T_c of YBa$_2$Cu$_3$O$_{7-\delta}$, and up to 164 K under 30 GPa pressure[2]. However very few spectroscopic studies have been carried out on this material [3–12] due to the difficulty to grow large enough single crystals with high optical quality surface. Working on the highest-T_c cuprate superconductor could therefore give us the chance to understand what gives rise to such a high T_c. Although the earlier Raman measurements on Hg-1223 suggested a multicomponent anisotropic superconducting (SC) gap (with two distinct gap maxima) [8, 9, 13], it turned out that the experimental findings were more appropriately described by a d-wave pairing gap [10–12]. The d-wave SC gap amplitude is expected to be maximum near the principal axes of the Brillouin zones (($\pm\pi$, 0) and (0, $\pm\pi$)), called the anti-nodal regions, while it is expected to vanish near the diagonal of the Brillouin zone ($\pm\pi/2, \pm\pi/2$), called the nodal regions [14, 15].

Here we present new electronic Raman scattering studies on Hg-1223, which greatly improve our previous results (fifteen years ago) [5, 8, 9, 11] by investigating the Raman spectra over a significantly wider energy range and revealing spectral features previously overlooked. We have performed both in and out of plane polarization Raman study on slightly under-doped Hg-1223 (T$_c$=122 K). In the (ab) plane we focus on the B_{1g}, B_{2g} and A_{1g} symmetries, which allow us to probe respectively the anti-nodal region, the nodal region and the whole Bril-

louin zone in the (k_x, k_y) plane. We find that the maximum amplitude of the pairing gap was underestimated in our previous work [5, 8, 9, 11], resulting much higher in energy at 1135 cm^{-1} (14 k_BT$_c$) instead of 800 cm^{-1} (9 k_BT$_c$).

We reveal a weakly temperature-dependence of the pairing gap 2Δ on a large temperature-range up to T_c. We also show that the pairing gap is associated with a peak-dip-hump structure in the Raman response, similarly to what observed by angle resolved photo-emission spectroscopy (ARPES) in Bi-2212 [16, 17]. Moreover we find two other distinct energy scales in B_{2g} symmetry and A_{1g} symmetry which disappear above T_c. The energy ratio between the B_{1g} and B_{2g} peaks is extremely high $\approx$ 2.6 in comparison with what we expect for a standard d-wave SC gap ($\approx$ 1.3) [18]. Using light polarizations along the c-axis we have also probed the A_{1g} and E_g symmetries. Interestingly, we detect in A_{1g} symmetry the same pairing peak at 1135 cm^{-1} as the one found in the (ab) plane with the B_{1g} symmetry. This shows that the c-axis electronic properties and the antinodal ones within the (ab) plane are tightly connected.

II. DETAILS OF THE EXPERIMENTAL PROCEDURE

The measurements have been performed on slightly underdoped (UD) Hg-1223 single crystal grown by a single step synthesis [19]. The single crystal is a parallelepiped with 0.9×0.9 mm^2 cross section and thickness 0.2 mm (see inset of fig.1). The c-axis is normal to the surface with the a-b plane directions 45° from the two larger edges. In order to have high optical quality surface, the sample has been polished using diamond

paste at $1/10$ μm. Dc magnetization measurements under field cooling (FC) and zero field cooling (ZFC) are displayed in fig.1. The T_c onset is estimated at 122 K with a middle transition at 117 K. The diamagnetic transition width is $\approx 6K$. The relatively large transition width might reflect slightly doping inhomogeneity [20].
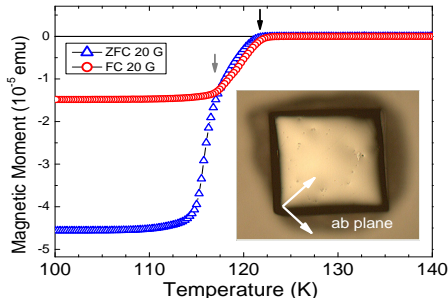

FIG. 1. Zero field cooling and field cooling magnetizations of under-doped Hg-1223. The applied magnetic field is perpendicular to the (ab) plane and its magnitude is of ≈ 20 $Gauss$. The black and grey arrows indicate respectively the T_c onset and the middle of the transition.

Raman experiments have been carried out using a JY-T64000 spectrometer in single grating configuration using a 600 grooves/mm grating and a Thorlabs NF533-17 notch filter to block the stray light. The spectrometer is equiped with a nitrogen cooled back illuminated 2048x512 CCD detector. We use the 532 nm excitation line from a diode pump solid state with laser power maintained at 4 mW. Measurements between 10 and 290 K have been performed using an ARS closed-cycle He cryostat. This configuration allows us to cover a wide spectral range (90 cm^{-1} to 4700 cm^{-1}) with a resolution sets at 5 cm^{-1}. The complete spectrum for B_{1g} symmetry is a recombination of three frames centered at different energies. Spectra for other symmetries have been obtained in one frame. Each frame is repeated twice to eliminate cosmic spikes and acquisition time ranged from 5 to 15 minutes. For comparison, in our initial study [8, 9, 11] we took almost a day to acquire a spectrum up to 1000 cm^{-1}. All the spectra have been corrected for the Bose factor and the instrumental spectral response. They are thus proportional to the imaginary part of the Raman response function $\chi''(\omega, T)$. Two sets of experimental configurations have been used. In the first set-up the direction of incident electric field is contained in the (ab) plane. The B_{1g} and $A_{1g}+B_{2g}$ geometries are obtained from crossed and parallel polarizations, respectively, along the Cu-O bond directions. Then, the crystal is rotated by $45°$ using a Attocube piezo-rotator ANR 101 to obtain the B_{2g} and $A_{1g}+B_{1g}$ geometries from crossed and parallel polarizations respectively. The A_{1g} , B_{1g} and B_{2g} symmetries are related to the x and y-components of the Raman susceptibility tensor. In the second set-up, the direction of the incident electric field is out of the (ab) plane (along the c-axis). This gives access to the A_{1g} and E_g symmetries related to the z and x components of the Raman susceptibility tensor.

III. EXPERIMENTAL RESULTS

In fig.2(a) is displayed the temperature dependence of the B_{1g} Raman response $\chi''_{B_{1g}}(\omega, T)$ of the UD Hg-1223 single crystal up to $T_c= 122$ K. We clearly observe the superconducting gap which manifests itself as a relatively sharp quasiparticle pair breaking peak at $2\Delta \approx 1135$ cm^{-1} and with a full width at half maximum of ≈ 150 cm^{-1} (see inset). The pairing-gap peak growth with decreasing T, from the normal to the superconducting state, is associated with the redistribution of the low energy electronic background from below to above ≈ 800 cm^{-1}. Interestingly, the pair breaking peak in the SC state is followed by a dip in the electronic continuum around 1600 cm^{-1} and a broader hump. The normal (122 K) and superconducting (13 K) electronic background finally merge near 2500 cm^{-1}.

In fig.2 (b) we display the superconducting B_{1g} Raman responses versus temperature subtracted from the normal one at T_c, $\chi''_{B_{1g}}(\omega, T) - \chi''_{B_{1g}}(\omega, T_c)$. As the temperature decreases we clearly see the growth of the pairing-gap peak at 1135 cm^{-1}. Notice a weak bump around 800 cm^{-1} which was previously erroneously interpreted as the 2Δ pairing peak [8, 9, 11]because of the short frequency range (≈ 1000 cm^{-1}) available. Above the pairing gap we detect a dip at 1577 cm^{-1} and a hump in the electronic background around 2500 cm^{-1}. The dip developps immediately below T_c as the pairing peak starts to grow. We find $\omega_{dip}/2\Delta \approx 1.4$. This structure has to be compared to the peak-dip-hump reported by ARPES in the spectral function of Bi-2212 at $(0,\pi)$ point [16, 17, 21, 22]. Although the electron Raman scattering is a two particles probe and ARPES is a single particle probe, both techniques may be revealing the same electronic structure. The peak-dip-hump structure observed in Bi-2212 by ARPES is still a matter of debate. Is it due to an electronic band structure effect or a collective mode ? [23]. The question is still open. It was first interpreted as a bosonic mode due to the coupling between spin fluctuations and electrons [24] and theoretical Raman investigations suggested that the predominantly linear low frequency dependence of the B_{1g} Raman response (see fig.2 (a)) and the dip just above the pairing peak hinted at a strong fermionic interaction with spin fluctuations [25]. These features deserve future deeper investigations.

The temperature dependence of the SC pairing gap is displayed in fig.2(c). The critical temperature is sufficiently high to give us an accurate estimate of the the pairing gap energy versus temperature. It appears that the temperature evolution of the pairing gap significantly differs from the one expected for a $d-$wave superconducting gap at the antinodes in a weak coupling limit[26].
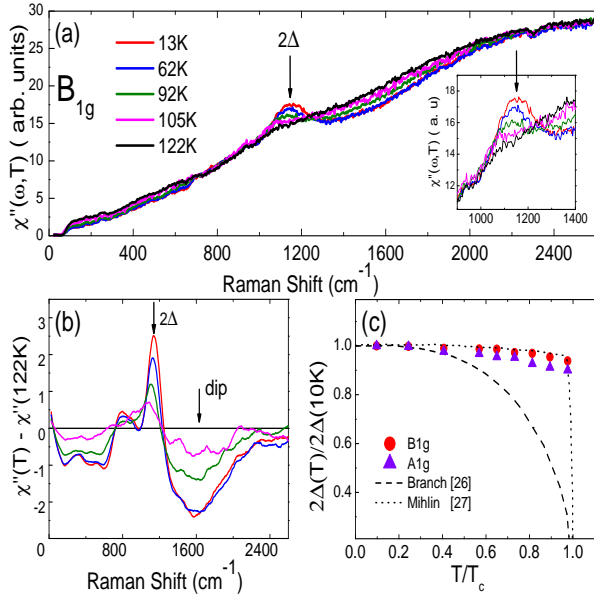
FIG. 2. (a) Temperature dependence of the B_{1g} Raman Response up to T_c for the under-doped Hg-1223 single crystal (T_c = 122K). The 2Δ pairing peak is detected at $\approx 1135\ cm^{-1}$. (b) Subtraction of the B_{1g} Raman Responses from the one at T_c = 122K. A peak -dip-hump structure can be observed. (c) Temperature dependence of the pairing gap detected in B_{1g} and A_{1g} symmetries. Its energy remains almost constant up to T_c for both symmetries. The dashed and dotted lines correspond respectively to the temperature evolution of a d-wave gap in a weak coupling limit and an order parameter for charge lattice bosons calculation (see text).

The trapezoidal shape is more relevant with a model of charge lattice bosons justified in the strong coupling and short coherence length limit [27–29]. Such a behavior for the SC gap was also reported by Raman scattering in one and two-copper-oxide-layer compounds slightly underdoped [30, 31]. At low temperature (13 K) we estimate the pairing gap at 14 $k_B T_c$ much higher than 4.28 $k_B T_c$ expected in the weak coupling limit. This hints at a strong coupling nature for the pairing state. Our findings about the pairing gap energy are in agreement with earlier tunneling and optical measurements on Hg-1223 compounds [10, 12]. In tunneling, the gap for an optimally doped Hg-1223 was estimated close to $\sim 13\ k_B T_c$ and a d-wave gap was successfully considered for interpreting the data. In optical conductivity, the pairing gap deduced from the scattering rate was estimated of about 1100 cm^{-1} i.e $\sim 13\ k_B T_c$.

In fig.3 are reported the Raman spectra obtained from light polarizations in the (ab) plane. The temperature dependencies of the Raman responses $\chi''_\nu(\omega, T)$ for ν = $B_{1g}, B_{2g}, A_{1g} + B_{1g}, A_{1g} + B_{2g}$ symmetries are displayed up to T_c. The Raman spectra in B$_{1g}$ and B$_{2g}$ symmetries (panels (a) and (b)) are free of phonon structures. This allows us to study the electronic background in a reliable way. In the A$_{1g}$+B$_{1g}$ and A$_{1g}$+B$_{2g}$ spectra (panel (c) and (d)), we observe sharp intensive phonon lines at 256,

380 and 591 cm^{-1}. A broader peak is detected at higher energy close to 1180 cm^{-1} which might reflect a double phonon structure stemming from the 591 cm^{-1} phonon line.
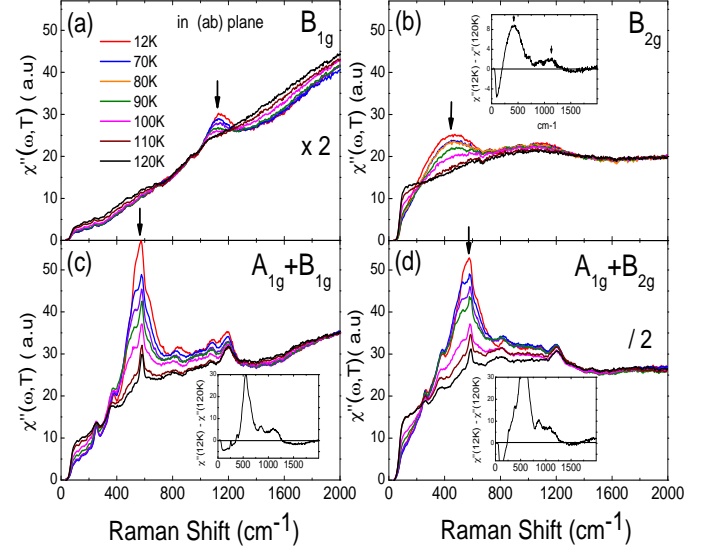

FIG. 3. Temperature dependencies of the Raman responses in (a) B_{1g}, (b) B_{2g}, (c) $A_{1g}+B_{2g}$ and (d) $A_{1g}+B_{1g}$ symmetries obtained from (ab) plane polarizations. The three distinct energy scales can be respectively seen in B_{1g}, B_{2g} and A_{1g} at 1135, 430 and 555 cm^{-1}. The insets display the subtracted Raman response between the superconducting (12 K) and the normal (122 K) ones. The insets of panels (c) and (d) have the same intensity scales to facilitate the comparison between the strength of the dip in the electronic continuum.

Focusing on the electronic background we detect three distinct electronic peaks in the SC state of Hg-1223 depending on the symmetry. The peak at 1135 cm^{-1} detected in the B_{1g} spectrum (panel (a)) has already been assigned to the d-wave pairing gap (see above). In B_{2g} spectrum (panel (b)) we observe a broad electronic peak at 430 cm^{-1}, whose full width at half maximum (FWHM) is $\approx$ 2.5 larger than the B_{1g} peak (see inset), and a small bump around 1135 cm^{-1}. We can see that the intensity of the B_{2g} superconducting peak is stronger than the B_{1g} one. This has already been observed for underdoped mercurate compounds [32]. The d-wave gap amplitude is maximum at the antinodes (B_{1g} symmetry) while it vanishes at the nodes (B_{2g} symmetry). Therefore, as expected, the energy of the B_{1g} peak is larger than the B_{2g} one. However the energy ratio between the B_{1g} and B_{2g} peak energies is particularly high $\approx$ 2.6. This is hard to reconcile with a d-wave SC gap which develops on a full cylindrical Fermi surface as in this picture the ratio would be close to 1.3 [18]. A possible explanation is to consider the formation of Fermi arcs [33], with a quasiparticles spectral weight mostly concentrated around the nodal regions. This can push the B_{2g} peaks to lower energy, as discussed in previous works [15, 34–37] and explain such a high B_{1g} /B_{2g} energy ratio.

In the $A_{1g} + B_{1g}$ spectrum (panel (c)) we also observe an intense SC electronic peak at 555 cm^{-1} (called the A_{1g} peak) whose FWHM is sharp enough (unlike the B_{2g} one) to track its temperature evolution (see fig. 2 (a)). It shifts slowly toward low energy as the temperatures raises in a similar way to the B_{1g} pairing peak. This hints that the A_{1g} peak is connected to the 2Δ pairing peak. In other hole-doped cuprates such as Bi-2212, the A_{1g} peak exhibits the same doping dependence than the B_{1g} pairing peak [38]. These results suggest that the A_{1g} peak is likely connected to a collective mode located below the 2Δ- threshold of the particle-hole continuum [39–42]. The A_{1g} peak detected in the $A_{1g} + B_{2g}$ spectrum (fig.3(d)) has a FWHM much larger than the one in the $A_{1g} + B_{1g}$ spectrum (fig.3(c)). This is due to the additional broadening stemming from the B_{2g} peak which is $\approx$ 2.5 larger than the one of the B_{1g} peak [43].

We have found in fig.2 (b) that the electronic background of the B_{1g} spectrum exhibits in the SC state a dip centered $\approx$ 1577 cm^{-1} just above the pairing gap. We can now estimate (from the subtracted Raman responses in fig.2 (b) and in the inset of fig.3 (b)) that the dip magnitude is higher by a factor of 4 in the B_{1g} spectrum in comparison with the B_{2g} one. The same effect in the dip magnitude is also observed between the $A_{1g} + B_{1g}$ and $A_{1g} + B_{2g}$ spectra. See for comparison insets of fig.3 (c) and (d). This confirms that the dip is a characteristic feature of the B_{1g} Raman spectra and mainly relevant to antinodal electronic properties as also noticed in Bi-2212 [23].

We finally turn to the Raman measurements with light polarization perpendicular to the (ab) plane i.e: along the c-axis. In fig.4 are displayed the Raman spectra in A_{1g} and E_g symmetries which correspond respectively to parallel and crossed polarizations (cf. experimental procedures). In A_{1g} symmetry (panels (a) and (b)), we detect a huge phonon line at 585 cm^{-1} with a shoulder at 534 cm^{-1}. These peaks are respectively assigned to the vertical motions of the apex oxygen atoms in the BaO plane and interstitial oxygen atoms in the HgO plane [5–7, 13]. The very strong Raman activity of the 585 cm^{-1} mode can be explained by (i) the polarizability enhancement due to the same direction of the atomic motions and the electric field along the c-axis and (ii) the phonon lifetime increasing along the c-axis due to the loss quasiparticle spectral weight perpendicular to the (ab) plane. Indeed the temperature dependence of the c-axis resistivity exhibits a semiconductor like behavior unlike the (ab) plane resistivity (which exhibits a metallic one) and a strong anisotropy $\rho_c \approx$ 1000 ρ_{ab} [44]. Although the electronic continuum is weaker along the c-axis than in the (ab) plane, we detect in A_{1g} symmetry (panel (b)) a redistribution of the electronic background from low to high energy and the growth of the pairing gap as the temperature decreases below T_c . After subtracting the A_{1g} normal Raman response at 130 K from the superconducting one at 10 K, (see inset of panel (b)), we find a
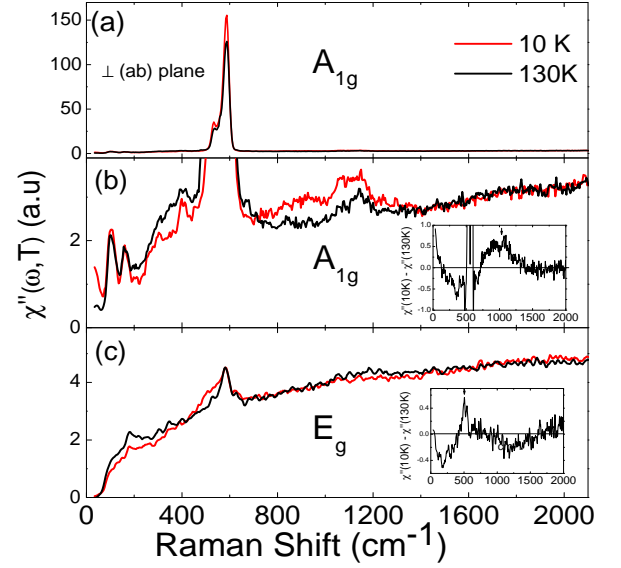

FIG. 4. Superconducting and normal Raman responses in (a, b): A_{1g} and (c): E_g symmetries obtained from c-axis polarizations

SC peak at 1135 cm^{-1}, i.e. the same energy of the pair breaking peak detected in B_{1g} symmetry (see fig.3 (a)). Probing the quasiparticles dynamics along the c-axis is thus equivalent to probe the B_{1g} quasi-particles dynamics in the (ab) plane. This can be understood by noticing that the square of the B_{1g} Raman vertex $(cosk_x - cosk_y)^2$ has the same symmetry as the c-axis hopping [45]. Our results confirm the close relationship between the antinodal electronic properties in the (ab) plane and the c-axis ones. In E_g symmetry (panel (c)) the subtraction of the normal to the superconducting Raman responses reveals a weak SC peak around 555 cm^{-1} close in energy to the one already detected in A_{1g} symmetry (see fig.3 (c)).

In conclusion, by performing electronic Raman scattering on Hg-1223 single crystal over a wide energy range we reveal spectral features previously overlooked. We succeeded to detect three distinct SC electronic peaks at 1135, 555 and 430 cm^{-1} respectively in the B_{1g} , A_{1g} and B_{2g} symmetries, obtained from in and out of plane polarizations. The 1135 cm^{-1} peak is assigned to the d-wave pairing gap at the antinodes. Its huge energy value $\approx$ 14 $k_B T_c$ and its weak temperature dependence below T_c hints at a strong coupling pairing state. Remarkably the 1135 cm^{-1} peak is also detected in A_{1g} symmetry along the c-axis which confirms the intimate connection between the quasiparticles dynamics at the antinodes within the (ab) plane and along the c-axis in the SC state. Finally, we find that the 1135 cm^{-1} superconducting peak displays a peak-dip-hump structure in the electronic background of the antinodal Raman spectrum similar to the one detected by ARPES in Bi-2212. Identify its origin requires a more deeper study which will be addressed in a near future.

[1] A. Schilling, M. Cantoni, J. D. Guo, and H. R. Ott, Nature **363**, 56 (1993).

[2] L. Gao, Y. Y. Xue, F. Chen, Q. Xiong, R. L. Meng, D. Ramirez, C. W. Chu, J. H. Eggert, and H. K. Mao, Phys. Rev. B **50**, 4260 (1994).

[3] Y. Ren, H. Chang, Q. Xiong, Y. Wang, Y. Sun, R. Meng, Y. Xue, and C. Chu, Physica C: Superconductivity **217**, 273 (1993).

[4] I.-S. Yang, H.-G. Lee, H.-S. Shin, J.-H. Park, S.-I. Lee, and S. Lee, Physica C: Superconductivity **222**, 386 (1994).

[5] A. Sacuto, A. Lebon, D. Colson, A. Bertinotti, J.-F. Marucco, and V. Viallet, Physica C: Superconductivity **259**, 209 (1996).

[6] X. Zhou, M. Cardona, C. W. Chu, Q. M. Lin, S. M. Loureiro, and M. Marezio, Phys. Rev. B **54**, 6137 (1996).

[7] X. Zhou, M. Cardona, D. Colson, and V. Viallet, Phys. Rev. B **55**, 12770 (1997).

[8] A. Sacuto, R. Combescot, N. Bontemps, P. Monod, V. Viallet, and D. Colson, EPL (Europhysics Letters) **39**, 207 (1997).

[9] A. Sacuto, R. Combescot, N. Bontemps, C. A. Müller, V. Viallet, and D. Colson, Phys. Rev. B **58**, 11721 (1998).

[10] J. Y. T. Wei, C. C. Tsuei, P. J. M. van Bentum, Q. Xiong, C. W. Chu, and M. K. Wu, Phys. Rev. B **57**, 3650 (1998).

[11] A. Sacuto, J. Cayssol, P. Monod, and D. Colson, Phys. Rev. B **61**, 7122 (2000).

[12] J. J. McGuire, M. Windt, T. Startseva, T. Timusk, D. Colson, and V. Viallet-Guillen, Phys. Rev. B **62**, 8711 (2000).

[13] X. Zhou, M. Cardona, D. Colson, and V. Viallet, Physica C: Superconductivity **282287, Part 2**, 1007 (1997), proceedings of the International Conference on Materials and Mechanisms of Superconductivity High Temperature Superconductors V Part {II}.

[14] T. P. Devereaux and R. Hackl, Rev. Mod. Phys. **79**, 175 (2007).

[15] A. Sacuto, Y. Gallais, M. Cazayous, M.-A. Méasson, G. D. Gu, and D. Colson, Reports on Progress in Physics **76**, 022502 (2013).

[16] A. V. Fedorov, T. Valla, P. D. Johnson, Q. Li, G. D. Gu, and N. Koshizuka, Phys. Rev. Lett. **82**, 2179 (1999).

[17] J. C. Campuzano, H. Ding, M. R. Norman, H. M. Fretwell, M. Randeria, A. Kaminski, J. Mesot, T. Takeuchi, T. Sato, T. Yokoya, T. Takahashi, T. Mochiku, K. Kadowaki, P. Guptasarma, D. G. Hinks, Z. Konstantinovic, Z. Z. Li, and H. Raffy, Phys. Rev. Lett. **83**, 3709 (1999).

[18] T. P. Devereaux, Phys. Rev. Lett. **74**, 4313 (1995).

[19] D. Colson, A. Bertinotti, J. Hammann, J. Marucco, and A. Pinatel, Physica C: Superconductivity **233**, 231 (1994).

[20] A. Bertinotti, D. Colson, J. Hammann, J.-F. Marucco, D. Luzet, A. Pinatel, and V. Viallet, Physica C: Superconductivity **250**, 213 (1995).

[21] T. Sato, H. Matsui, S. Nishina, T. Takahashi, T. Fujii, T. Watanabe, and A. Matsuda, Phys. Rev. Lett. **89**, 067005 (2002).

[22] I. M. Vishik, W. S. Lee, R.-H. He, M. Hashimoto, Z. Hussain, T. P. Devereaux, and Z.-X. Shen, New Journal of Physics **12**, 105008 (2010).

[23] A. Damascelli, Z. Hussain, and Z.-X. Shen, Rev. Mod. Phys. **75**, 473 (2003).

[24] M. Eschrig and M. R. Norman, Phys. Rev. Lett. **85**, 3261 (2000).

[25] A. Chubukov, D. Morr, and G. Blumberg, Solid State Communications **112**, 183 (1999).

[26] D. Branch and J. P. Carbotte, Phys. Rev. B **52**, 603 (1995).

[27] A. Mihlin and A. Auerbach, Phys. Rev. B **80**, 134521 (2009).

[28] E. Altman and A. Auerbach, Phys. Rev. B **65**, 104508 (2002).

[29] P. W. Anderson, Science **235**, 1196 (1987).

[30] W. Guyard, M. Le Tacon, M. Cazayous, A. Sacuto, A. Georges, D. Colson, and A. Forget, Phys. Rev. B **77**, 024524 (2008).

[31] T. Staufer, R. Nemetschek, R. Hackl, P. Müller, and H. Veith, Phys. Rev. Lett. **68**, 1069 (1992).

[32] M. Le Tacon, A. Sacuto, A. Georges, G. Kotliar, Y. Gallais, D. Colson, and A. Forget, Nat Phys **2**, 537 (2006).

[33] M. R. Norman, H. Ding, M. Randeria, J. C. Campuzano, T. Yokoya, T. Takeuchi, T. Takahashi, T. Mochiku, K. Kadowaki, P. Guptasarma, and D. G. Hinks, Nature **392**, 157 (1998).

[34] X. K. Chen, J. G. Naeini, K. C. Hewitt, J. C. Irwin, R. Liang, and W. N. Hardy, Phys. Rev. B **56**, R513 (1997).

[35] A. V. Chubukov and M. R. Norman, Phys. Rev. B **77**, 214529 (2008).

[36] J. P. F. LeBlanc, J. P. Carbotte, and E. J. Nicol, Phys. Rev. B **81**, 064504 (2010).

[37] S. Blanc, Y. Gallais, M. Cazayous, M. A. Méasson, A. Sacuto, A. Georges, J. S. Wen, Z. J. Xu, G. D. Gu, and D. Colson, Phys. Rev. B **82**, 144516 (2010).

[38] S. Benhabib, A. Sacuto, Y. Gallais, M. Cazayous, Y. Gallais, M. A. Méasson, R. D. Zhong, J. Schneeloch, G. D. Gu, D. Colson, and A. Forget, "Three energy scales in the superconducting state of hole-doped cuprates detected by electronic raman scattering," (2015).

[39] F. Venturini, U. Michelucci, T. P. Devereaux, and A. P. Kampf, Phys. Rev. B **62**, 15204 (2000).

[40] Y. Gallais, A. Sacuto, P. Bourges, Y. Sidis, A. Forget, and D. Colson, Phys. Rev. Lett. **88**, 177401 (2002).

[41] P. Bourges, B. Keimer, S. Pailhès, L. Regnault, Y. Sidis, and C. Ulrich, Physica C: Superconductivity **424**, 45 (2005).

[42] X. Montiel, T. Kloss, C. Pépin, S. Benhabib, Y. Gallais, and A. Sacuto, arXiv:1504.03951 (2015).

[43] Notice that the electronic background level of the $A_{1g}+B_{2g}$ spectrum below 1000 cm^{-1} is higher than the $A_{1g}+B_{1g}$ one. This is a consequence of a stronger Raman intensity of the B_{2g} peak compared to the B_{1g} one..

[44] A. Carrington, D. Colson, Y. Dumont, C. Ayache, A. Bertinotti, and J. Marucco, Physica C: Superconductivity **234**, 1 (1994).

[45] O. Andersen, A. Liechtenstein, O. Jepsen, and F. Paulsen, Journal of Physics and Chemistry of Solids **56**, 1573 (1995), proceedings of the Conference on Spectroscopies in Novel Superconductors.